ACS chemical biology

ARTICLE

A Minimal Peptide Sequence That Targets Fluorescent and Functional Proteins into the Mitochondrial Intermembrane Space

Takeaki Ozawa[†,‡,§], Yutaka Natori[†], Yusuke Sako[†], Haruko Kuroiwa[¶], Tsuneyoshi Kuroiwa[¶], and Yoshio Umezawa[†,*]

[†]Department of Chemistry, School of Science, The University of Tokyo, 7-3-1 Hongo, Bunkyo-ku, Tokyo 113-0033, Japan, [‡]Department of Molecular Structure, Institute for Molecular Science, 38 Nishigonaka, Myodaiji, Okazaki, Aichi 444-8585, Japan, [§]Precursory Research for Embryonic Science and Technology, Japan Science and Technology Agency, 4-1-8 Honcho Kawaguchi, Saitama 332-0012, Japan, and [¶]Department of Life Science, College of Science, Rikkyo University, Tokyo 171-8501, Japan

ABSTRACT Protein-based fluorescent and functional probes are widely used for real-time visualization, purification, and regulation of a variety of biological molecules. The protein-based probes can generally be targeted into subcellular compartments of eukaryotic cells by a particular short peptide sequence. Little is known, however, about the sequence that targets probes into the mitochondrial intermembrane space (IMS). To identify the IMS-targeting sequence, we developed a simple genetic screening method to discriminate the proteins localized in the IMS from those in the mitochondrial matrix, thereby revealing the minimum requisite sequence for the IMS targeting. An IMS-localized protein, Smac/DIABLO, was randomly mutated, and the mitochondrial localization of each mutant was analyzed. We found that the four residues of Ala-Val-Pro-Ile are required for IMS localization, and a sequence of these four residues fused with matrix-targeting signals is sufficient for targeting the Smac/DIABLO into the IMS. The sequence was shown to readily direct three dissimilar proteins of interest to the IMS, which will open avenues to elucidating the functions of the IMS in live cells.

*Corresponding author,
umezawa@chem.s.u-tokyo.ac.jp.

Received for review December 26, 2006
and accepted February 22, 2007.

Published online March 9, 2007

10.1021/cb600492a CCC: $37.00

© 2007 American Chemical Society

Mammalian mitochondria have pivotal roles in the production of most of the cellular ATP, generation of reactive oxygen species, calcium metabolism, and cell death. Such mitochondrial functions are closely related to the proteins in the structurally complex organelle. Most mitochondrial proteins are encoded by the nuclear genome and synthesized on cytosolic ribosomes. The proteins are then targeted into the mitochondria, where the proteins are sorted to one of the submitochondrial compartments, the outer and inner membranes and two aqueous compartments, the intermembrane space (IMS), and the matrix (*1*–*3*). The targeting and sorting into the mitochondrial matrix are achieved by N-terminal presequences of precursor proteins. The presequences are composed of 20–80 residues capable of folding into a positively charged amphipathic helix. The helix is recognized by specific receptors in the mitochondrial outer membrane and is then inserted into the inner membrane *via* the membrane potential. The energy generated from ATP hydrolysis by motor proteins in the matrix mediates completion of the translocation (*1*). In contrast, no uniform pathway exists into the mitochondrial IMS (*4*–*9*): although several different pathways have been proposed regarding the protein transport into the IMS, no signal sequence has been identified that allows exogenous proteins to locate in the IMS.

In the past decade, genetically encoded probes have often been used as powerful tools to image morphologies or ionic properties of intracellular organelles in living cells (*10*). In particular, custom-made fluorescent probes targeted into the organelles enabled real-time

and quantitative analyses of the pH (*11–13*), calcium ion (*14*), and redox potential (*15*). The targeting of the probes into particular organelles is generally achieved by the addition of a short signal peptide sequence to the probes of interest. Because of the ability of the signal sequences to deliver the probes exclusively into specific subcellular locations, they have also been used for intracellular antibodies (so-called intrabodies) as probes to regulate the function of target proteins in a specific organelle (*16–19*). The targeting of the probes was accomplished in such organelles as the nucleus, endoplasmic reticulum (ER), peroxisome, and mitochondrial matrix, but little was known about the IMS-targeting sequences. To elucidate crucial roles for cellular functions of the IMS, such as energy production, protein transport, and apoptosis, it is very important to identify the signal sequences that deliver a particular protein into the mitochondrial IMS.

A mammalian protein called Smac/DIABLO is an IMS-localized protein that is conserved in mammals (*20, 21*). The Smac/DIABLO protein derived from *Mus musculus* is synthesized as a precursor molecule of 237 amino acids; the N-terminal 53 residues serve as the mitochondrial targeting sequence, which is removed by the inner membrane peptidase (IMP) complex after import (*22*). Thus, the mature Smac/DIABLO protein has 184 amino acids, and the four residues of the N-terminus are Ala-Val-Pro-Ile. These four N-terminal residues play an indispensable role in Smac/DIABLO function; they promote apoptosis by eliminating the inhibitory effect of the inhibitor of apoptosis protein (IAP) through physical interaction (*23–25*). A point mutation in the four residues leads to a loss of interaction with IAP and a concomitant loss of the Smac/DIABLO function. The structural and functional aspects of Smac/DIABLO have been extensively investigated, but how the protein targets into the mitochondrial IMS remains unknown.

To identify the amino acids or domains of Smac/DIABLO important for targeting into the IMS, we have developed a high-throughput screening system that enables discrimination between the proteins in the IMS and those in the mitochondrial matrix or cytosol. Using this system, we identified from Smac/DIABLO mutant libraries the amino acids necessary for the localization of the IMS. We further showed that amino acid residues 54–57 (Ala-Val-Pro-Ile), which are crucial for the apoptotic function, are also important for the IMS localization. We found that N-terminal amino acid residues 10–57 (RSVCSLFRYRQRFPVLANSKKRCFSELIKPWHKTVLTGFGMTLCAVPI) are the minimal sequence that functions as the IMS-targeting signal. We demonstrated that this IMS-targeting signal is able to deliver different probe proteins and intrabodies into the IMS.

RESULTS AND DISCUSSION

Rapid Discrimination between Mitochondrial IMS- and Matrix-Localized Proteins. Because the diameter of the mitochondria is <1 μm, it is impossible to discriminate the proteins localized in the mitochondrial matrix from those in the IMS by immunostaining under the optical microscope. To date, discrimination of the protein sublocalization has therefore been determined by immunogold electron microscopy or mitochondrial subfractionation followed by immunoblot analysis (*26, 27*). Although these techniques are reliable and accurate, the sample preparation for electron microscopy requires many laborious steps, such as fixing the cells with resin, slicing them into thin sections, and blotting them with antibodies. Subfractionation techniques take a considerable amount of time because of the laborious electrophoresis, which limits screening and identification of the IMS-localized proteins. To bypass these steps, we developed a simple method to discriminate between the proteins localized in the mitochondrial IMS and those in the matrix or cytosol. The concept is based on reconstitution of split-enhanced GFP (split-EGFP) by protein splicing with a DnaE intein (Figure 1) (*28*). Protein splicing is a reaction in which an intein is excised from a polypeptide precursor and then the flanking polypeptides are linked by a native peptide bond (*29*). We previously developed a new split-EGFP reporter for identifying the mitochondrial-matrix-localized proteins (Figure 1, left) (*28*). The fluorescence of the split-EGFP reporter can be recovered by protein splicing when a protein transports into the mitochondrial matrix.

In the present study, we constructed a cell line in which C-terminal fragments of DnaE and EGFP are localized in the mitochondrial IMS (Figure 1, right). If a test protein fused to N-terminal fragments of EGFP and DnaE localizes in the mitochondrial IMS, then the N- and C-terminal fragments of DnaE are brought close enough to fold and initiate protein splicing. The N- and C-terminal fragments of EGFP are connected by a peptide bond, and fluorescence is recovered in the IMS. If a test protein localizes in the mitochondrial matrix, then the mitochondrial inner membrane separates the N-terminal

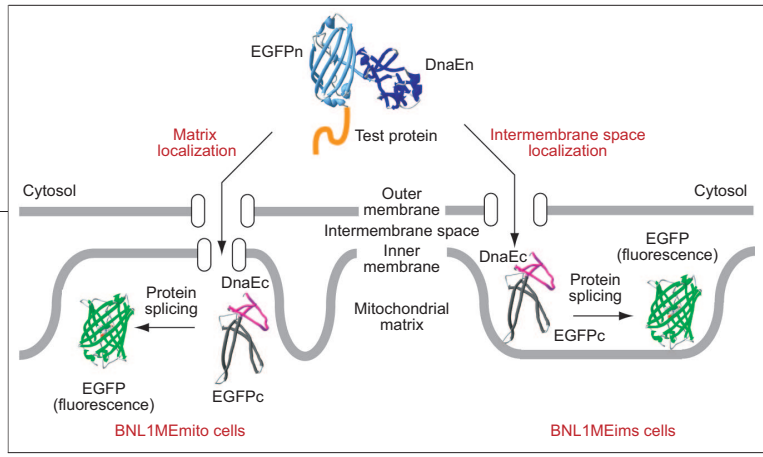

Figure 1. EGFP reconstitution by protein splicing in submitochondrial compartments. When a test protein is localized in the mitochondrial matrix (left) or in the IMS (right), N- and C-terminal DnaE are brought close together, and EGFP is formed by protein splicing in the respective compartments. BNL1MEmito cells permanently express a fusion composed of C-terminal fragments of DnaE and EGFP in the mitochondrial matrix (left), and BNL1MEims cells express the same fusion in the IMS (right). The blue and magenta 3D structures represent DnaEn and DnaEc, and the light blue and dark gray structures represent N- and C-terminal fragments of EGFP, respectively. The orange strand represents a test protein.

DnaE from the C-terminal DnaE, and no splicing reaction occurs.

To locate the fusion protein of C-terminal fragments of DnaE and EGFP (hereafter termed as DnaEc–EGFPc) in the mitochondrial IMS, a complementary DNA (cDNA) sequence of Smac/DIABLO was fused to the sequence encoding DnaEc–EGFPc with a flexible peptide linker (Supplementary Figure 1). The fusion proteins of Smac/DIABLO and DnaEc–EGFPc were expressed in a cultured cell (BNL1ME) derived from normal liver cells, and a stably expressed cell line designated BNL1MEims was prepared.

To examine the mitochondrial localization of Smac/DIABLO fused with DnaEc–EGFPc, we fractionated and treated mitochondria with a protease, trypsin. When intact mitochondria were isolated from BNL1MEims cells and treated with the protease, the Smac/DIABLO fused with DnaEc–EGFPc was not digested in the presence of trypsin, whereas translocase of the outer mitochondrial membrane 20 (Tom20), a mitochondrial outer-membrane marker (*30*), disappeared completely (Figure 2). When mitochondrial outer membrane was disrupted selectively by digitonin, the Smac/DIABLO and DnaEc–EGFPc fusion was completely digested by trypsin, together with an IMS marker, cytochrome *c* (Cyt*c*) (*31*). In contrast, mitochondrial heat shock protein (Hsp60), which is known as a matrix marker (*32*), was not digested under the same experimental conditions. When mitochondrial membrane was solubilized with a detergent, Triton X-100, all mitochondrial proteins, including Hsp60, were digested by trypsin. These results indicate that the fusion protein of Smac/DIABLO and DnaEc–EGFPc was targeted into the IMS.

To investigate whether protein splicing occurs in the mitochondrial IMS, we constructed a retroviral vector, pMX-Smac/ED–FLAG, which encodes the sequences of Smac/DIABLO, EGFPn–DnaEn, and FLAG epitope tag (Supplementary Figure 1). The vector was packaged into retroviruses, which were then used to infect BNL1MEims cells. Western blot analysis of the infected cells with GFP antibodies showed that protein splicing occurred in the BNL1MEims cells to produce a Smac–EGFP fusion protein (Figure 3, panel a, lane 3). Localization of the reconstituted EGFP was the same as that of mitochondria stained with tetramethylrhodamine ethyl ester (TMRE) (Figure 3, panel b), a confirmation that the splicing reaction and split-EGFP reconstitution occurred in mitochondria. To demonstrate that the splicing reaction is specific for IMS-localized proteins, we constructed two vectors, pMX-CaM (calmodulin)/ED–FLAG and pMX-MTS (mitochondrial targeting signal)/ED–FLAG (Supplementary Figure 1). In the case of pMX-CaM/ED–FLAG, a cytosolic protein, CaM, was fused with EGFPn–DnaEn, while the plasmid pMX-MTS/ED–FLAG contains a mitochondrial-matrix-targeting signal derived from subunit VIII of cytochrome *c* oxidase (*13*). No splicing product was observed when the EGFPn–DnaEn was targeted into the mitochondrial matrix or cytosol (Figure 3, panel a, lanes 2 and 4). These results indicated that the splicing product was generated only when EGFPn–DnaEn was targeted into the mitochondrial IMS.

Next, we assessed the fluorescence intensity of individual living cells by fluorescence-activated cell sorting (FACS). BNL1MEims cells infected with retroviruses encoding Smac/

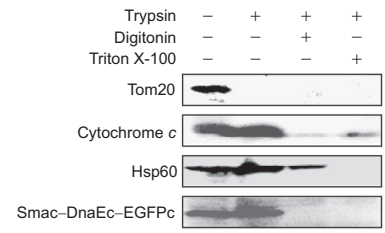

Figure 2. Subcellular localization of Smac/DIABLO connected to the C-terminal fragments of EGFP and DnaE. Mitochondrial outer membranes are disrupted by the addition of digitonin; therefore, only inner membrane and matrix proteins are collected and blotted with the indicated antibodies. The addition of Triton disrupted both the inner and outer mitochondrial membranes, and all proteins were digested. The blot was performed with the following antibodies: goat anti-Tom20 (Tom20), mouse anti-cytochrome *c* (Cytochrome *c*), mouse anti-Hsp60 (Hsp60), and mouse anti-GFP antibodies (Smac–DnaEc–EGFPc).

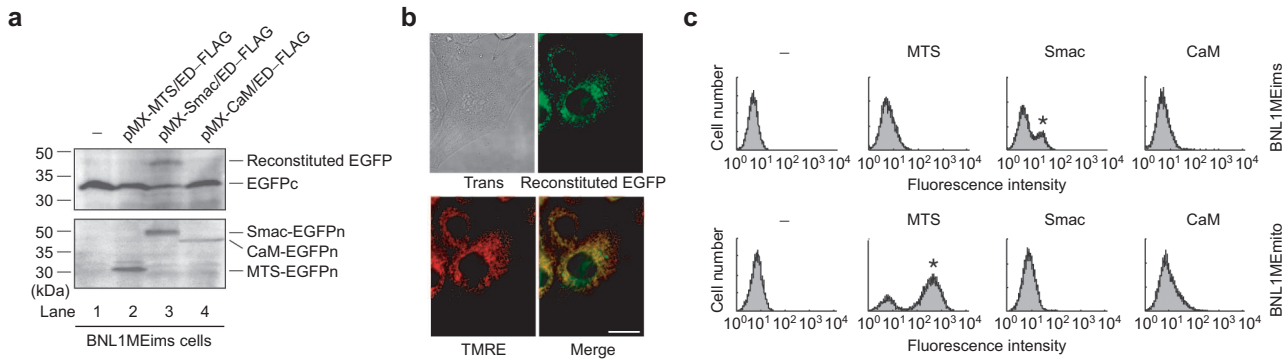

Figure 3. Selective reconstitution of EGFP in the mitochondrial IMS or matrix. a) Western blot analysis of the splicing reaction. Whole-cell lysates from BNL1MEims cells expressing EGFPn–DnaEn-tagged MTS, Smac/DIABLO, and CaM were analyzed by Western blot with monoclonal antibodies specific to the C-terminal half of EGFP (upper panel) and FLAG (lower panel). b) Expression of the Smac–EGFPn–DnaEn fusion in BNL1MEims cells and localization of reconstituted EGFP to mitochondria. BNL1MEims cells infected with retroviruses of pMX-Smac/ED–FLAG were cultured for 2 d, and the cells were spread on a glass-bottom dish. The fluorescence of reconstituted EGFP was recorded by a confocal microscope (spliced EGFP). After the image was taken, mitochondria were stained with TMRE. The superimposed image (Merge) shows the reconstituted EGFP localization specific to mitochondria. Trans = transmission image, bar = 10 μm. c) FACS analysis of BNL1MEmito and BNL1MEims cells harboring EGFPn–DnaEn fusion proteins. The cells were infected with retroviruses generated from pMX-MTS/ED–FLAG (MTS), pMX-Smac/ED–FLAG (Smac), or pMX-CaM/ED–FLAG (CaM). For comparison, uninfected cells are also shown (–). Asterisks (*) indicate a population of fluorescent cells.

DIABLO and N-terminal fragments of EGFP and DnaE showed a strong fluorescence (Figure 3, panel c). In contrast, no fluorescence was observed in the BNL1MEims cells when the EGFPn–DnaEn was targeted into the mitochondrial matrix or cytosol. In the case of a cell line of BNL1MEmito whose mitochondrial matrix harbors DnaEc–EGFPc, fluorescence was observed only when the EGFPn–DnaEn was targeted into the mitochondrial matrix. From these results combined with those of Western blot analysis, we concluded that the present N-terminal probe enables a rapid discrimination between the proteins targeted into the mitochondrial IMS and those targeted into the matrix by using the BNL1MEims and BNL1MEmito cells.

Identification of Amino Acid Sequences Required for IMS Localization. Random alteration of amino acids through random mutagenesis or the introduction of expression libraries reveals the roles of specific amino acids in the activity of proteins (*33, 34*). To investigate which amino acid residues are important for the IMS localization, we introduced random mutations into the cDNA sequences of Smac/DIABLO by the error-prone polymerase chain reaction (PCR) method (*35*). In this study, we created two mutation libraries at a rate of 0.42% and 1.1% point mutations, designated Smac(L)/ED–FLAG and Smac(H)/ED–FLAG, respectively. The libraries were packaged into retroviruses and infected into BNL1MEmito cells. When BNL1MEmito cells were infected with wild-type Smac/ED–FLAG, the cells showed no fluorescence (Figure 4). On the other hand, when the mutation libraries Smac(L)/ED–FLAG and Smac(H)/ED–FLAG were infected into the BNL1MEmito cells, 0.5% and 1.5% of total cells showed fluorescence. The results indicate that some mutations allowed localization of Smac/DIABLO mutants in the mitochondrial matrix.

To determine the mutated amino acid sequences that allow translocation into the mitochondrial matrix, we collected the fluorescent cells from the library-infected BNL1MEmito cells by FACS. The DNA of Smac/DIABLO mutants was extracted from each cloned cell, and the sequence was analyzed. Interestingly, we found that all the mutants have either a point mutation at Met50 replaced by lysine or Cys53 replaced by arginine (Table 1). To prove that only one point mutation in the amino acid sequences causes the mislocalization of Smac/DIABLO, we expressed a Smac/DIABLO mutant of M50K or C53R in either BNL1MEmito or BNL1MEims cells, and we used FACS to analyze fluorescence intensity of the individual cell. As expected, all the cells expressing the mutant Smac/DIABLO showed

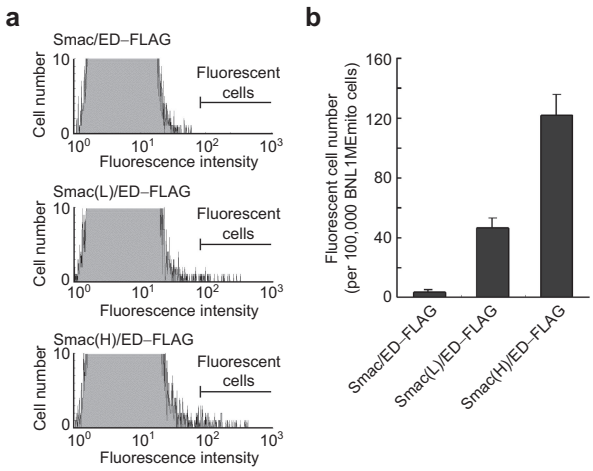

Figure 4. Analysis of the mitochondrial sublocalization with Smac/DIABLO mutation libraries. a) Enlarged FACS profiles. BNL1MEmito cells were infected with the cDNA retroviral libraries of Smac(L)/ED–FLAG or Smac(H)/ED–FLAG with an infection efficiency of 10%. After incubation, the cells were stripped off and analyzed by FACS. Histograms for the cells harboring wild-type Smac/DIABLO connecting EGFPn–DnaEn are given (Smac/ED–FLAG) to show the background fluorescence. b) The number of fluorescent cells infected with Smac/DIABLO mutation libraries. The number of fluorescent cells per 100,000 analyzed cells are shown.

a strong fluorescence in the mitochondrial matrix (Supplementary Figure 2); this confirmed that a single amino acid modification at Met50 or Cys53 resulted in changing the localization of Smac/DIABLO from the mitochondrial IMS to the matrix.

Met50 and Cys53 in Smac/DIABLO reside in the C-terminal end of the mitochondria-targeting presequence (amino acid residues 1–53), which includes a hydrophobic stretch between residues 43 and 53 (Supplementary Figure 3). This stretch may be important for the correct sorting of Smac/DIABLO to the mitochondrial IMS. To investigate the role of the hydrophobic sequences, we generated a series of Smac/DIABLO deletion mutants and fused them to the N-terminal fragments of EGFP and DnaE (Figure 5). These fusion proteins were expressed in both BNL1MEims and BNL1MEmito cells, and their fluorescence intensities were analyzed. No fluorescence was observed in the case of BNL1MEims cells expressing Smac(1–44)/ED–FLAG (Smac(1–44) denotes amino acids 1–44 from the N-terminus), whereas the BNL1MEmito cells expressing Smac(1–44)/ED–FLAG exhibited a strong fluorescence. These results indicated that Smac(1–44)/ED–FLAG was predominantly localized in the mitochondrial matrix. Next, the presequence of the MTS in Smac/DIABLO (Smac(1–53)/ED–FLAG), which contains the hydrophobic stretch, was expressed in the BNL1MEims and BNL1MEmito cells. We found that the presequence of Smac/DIABLO works as a mitochondrial-matrix-targeting sequence. When the presequence was extended with alanine (Smac(1–54)/ED–FLAG) or Ala-Val (Smac(1–55)/ED–FLAG), the sequence was also found to lead the N-terminal fragments of EGFP and DnaE into the mitochondrial matrix. In contrast, addition of Ala-Val-Pro to the presequence resulted in a marked decrease in the fluorescence intensity of BNL1MEmito cells, whereas the population of fluorescent cells in the BNL1MEims increased. The fluorescence of the

TABLE 1. Summary of the mutated amino acids in Smac/DIABLO

Mutant no.	Mutated amino acids[a]	Clone no.[b]
Smac(L)/ED–FLAG		
Smac-m1	*M50K*	1
Smac-m2	*C53R*	2
Smac-m3	*M50K*, L52P, H171R	1
Smac-m4	R17K, *C53R*	6
Smac-m5	*C53R*, Q59R, Q219P, S222G, R235C	10
Smac-m6	*C53R*, K121R, Q145R, V195M, E208G, Q216L	1
Smac(H)/ED–FLAG		
Smac-m7	A2V, C13Y, *C53R*, K150R	4
Smac-m8	*M50K*, V76A, I95T, S110P, Q171H	5
Smac-m9	R38K, H41R, *C53R*, A97V, L108S, Q132R, Y233S	1

[a]Met encoded in the start codon ATG is defined as the amino acid position 1. Then the presequence of the mitochondrial targeting presequence is numbered from 1 to 53, and the mature Smac/DIABLO after cleavage of the presequence is from 54 to 237. Mutations of M50K and C53R are highlighted in italic type. [b]Clone no. indicates multiplicity of the analyzed clones.

BNL1MEmito cells completely disappeared when four residues (Ala-Val-Pro-Ile) were added to the presequence. When the four residues were deleted from the full-length Smac/DIABLO, the BNL1MEims cells showed no fluorescence. From these analyses, we concluded that the four N-terminal residues Ala-Val-Pro-Ile are necessary for IMS localization.

To identify a minimal sequence that targets Smac/DIABLO into the mitochondrial IMS, we generated a series of N-terminal deletion mutants and analyzed their localizations in mitochondria (Supplementary Figure 4). BNL1MEims cells expressing Smac(5–57)/ED–FLAG and Smac(10–57)/ED–FLAG showed strong fluorescence, an indication that deletion of four or nine amino acid residues from the amino terminus has no effect on the ability of the signal sequence to target the EGFPn–DnaEn to the IMS. The fluorescence intensity of BNL1MEims cells expressing Smac(11–57)/ED–FLAG was quite weak, and the fluorescence of BNL1MEims cells expressing Smac(12–57)/ED–FLAG completely disappeared. When amino acid residues 10, 11, 12, 13, 14, 15, 16 and 28 were deleted from the amino terminus of the signal sequence, BNL1MEims cells including these signal sequences also showed no fluorescence. We concluded that amino acids 10–57 (RSVCSLFRYRQRFPVLANSKKRCFSELIKPWHKTVLTGFGMTLC-AVPI), which include the Ala-Val-Pro-Ile motif, sufficiently target Smac/DIABLO to the mitochondrial IMS and the sequence cannot be further shortened without losing its targeting ability.

General Applicability of the Signal Sequence Targeting to the Mitochondrial IMS. We investigated whether the N-terminal 57 residues, including Ala-Val-Pro-Ile, in Smac/DIABLO are generally able to lead a particular protein into the IMS. To demonstrate this, we engineered the cDNA that encoded a pH indicator, a yellow-emission variant of GFP (YFP(H148G)) (*36*), to contain the signal sequence of the IMS and expressed it in cultured mammalian cells. We generated NIH3T3 cells expressing the signal-sequence-connected YFP(H148G) by infecting the cells with retroviruses at an infection efficiency of 30%. A microscopic analysis revealed that YFP(H148G) was exclusively localized in mitochondria (Supplementary Figure 5, panel a). Next, we investigated localization of YFP(H148G) in the submitochondrial compartments (Supplementary Figure 5, panel b). Isolation of mitochondria from NIH3T3 cells showed that YFP(H148G) connected with the 57 amino

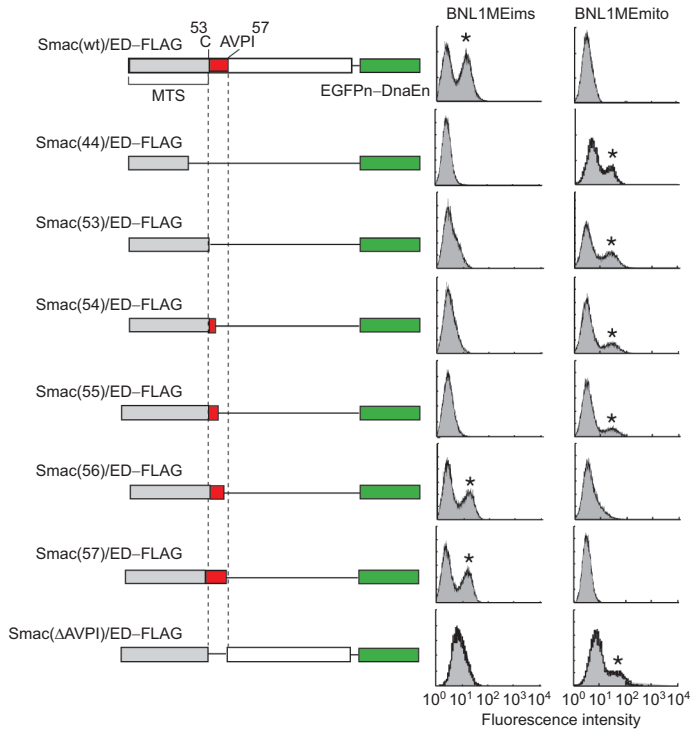

Figure 5. Analysis of truncation and internal deletion mutants of Smac/DIABLO. The numbers of amino acid sequences of Smac/DIABLO are indicated in parenthesis. Smac(ΔAVPI) represents the construct of Smac/DIABLO with four amino acids, Ala-Val-Pro-Ile, deleted. Constructs shown as dark boxes are the mitochondrial presequence of Smac/DIABLO. Constructs shown in white boxes are the sequence of Smac/DIABLO, and its amino-terminal four residues are red. The sequences of truncation and internal deletion mutants are connected with those of EGFPn–DnaEn (green boxes), and retroviruses containing the sequence were used to infect BNL1MEims and BNL1MEmito cells. Asterisks (*) indicate a population of fluorescent cells.

acid residues remained resistant to protease digestion with trypsin. However, the YFP(H148G) was mostly degraded when the outer membrane was permeabilized with digitonin, a strong indication that YFP(H148G) is predominantly localized in the IMS. In contrast, the YFP(H148G) targeted into the mitochondrial matrix is not degraded, a sign that the inner membrane remained intact. To examine whether the YFP(H148G) is anchored in the mitochondrial inner membrane or moves freely in the IMS, we ruptured the mitochondrial outer membrane by inducing apoptosis. When YFP(H148G) was connected with the IMS signal sequence or full-length Smac/DIABLO, stimulation of the HeLa cells (derived from human carcinoma of cervix) or MCF-7 cells (de-

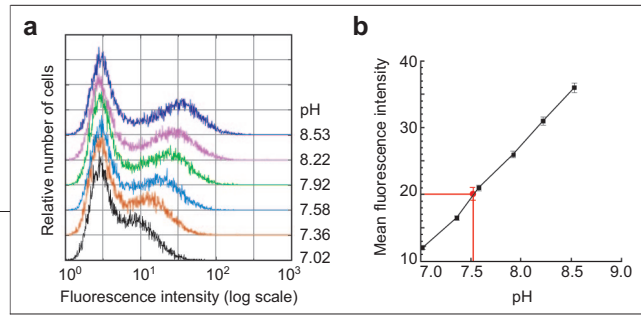

Figure 6. Targeting YFP(H148G) into the IMS. a) Measurement of pH in the IMS. Fluorescence intensity of the cells containing YFP(H148G) was analyzed for different pH values by FACS. Signal-sequence-tagged YFP(H148G) was expressed in the NIH3T3 cells, and the cells were incubated with ionophores at the indicated pH values. Infection efficiency of retroviruses was controlled at 30%. b) Determination of pH in the IMS. The figure is a standard curve derived from the histogram (panel a), showing a mean fluorescence intensity in the population of the fluorescent cells. The measurements were repeated three times for each pH value, and the results were indicated as mean ± SD. A closed circle in red shows a mean fluorescence intensity of the NIH3T3 cells expressing signal-sequence-tagged YFP(H148G). The pH value estimated by YFP(H148G) is 7.5.

rived from human breast cancer) with staurosporine (STS) resulted in the release of the YFP(H148G) from the IMS into the cytosol (Supplementary Figure 6). In the case of YFP(H148G) targeted into the matrix, no change in the localization of YFP(H148G) was observed. These results demonstrate that the signal sequence of the mitochondrial IMS has the ability to accurately lead the exogenous indicator into the mitochondrial IMS and to allow the indicator to diffuse freely inside the organelle.

To determine the pH in the IMS, we measured the fluorescence intensity of YFP(H148G) with differing pH. The cells expressing YFP(H148G) were incubated with ionophores of nigericin and monensin and then equilibrated in buffers of differing pH. FACS analysis showed an almost linear increase in fluorescence over the pH range from 7.0 to 8.5 (Figure 6, panels a and b). Using this calibration, we extrapolated the pH value of the IMS targeted with the YFP(H148G) from the fluorescence intensity of the cells without the ionophore. The pH was estimated at 7.5 when the cells were in a resting state, consistent with previous reports of a pH value in the IMS (*37*).

To further explore general applicability of the IMS-targeting sequence, we examined whether this can deliver several proteins with different features into the IMS. To this end, we tested a FRET-type Ca^{2+} indicator (cameleon) (*38*) and a redox indicator (roGFP) (*15*), because these proteins are useful for examining the temporal changes of Ca^{2+} concentrations and redox potential in the IMS. We also tested an antibody of scFv (single-chain variable fragments) that is useful for isolating protein complexes from crude cell lysates. These proteins were connected with the IMS-targeting sequence, the N-terminal 57 amino acids of Smac/DIABLO, and were expressed in BNL1ME cells. Analysis with fluorescence microscopy revealed that all the proteins were targeted into the mitochondria (Figure 7). Next, we examined the localization of submitochondrial compartments with subfractionation techniques. In the control experiments, the proteins connected with the N-terminal 53 amino acids, which work as a matrix-targeting sequence, were

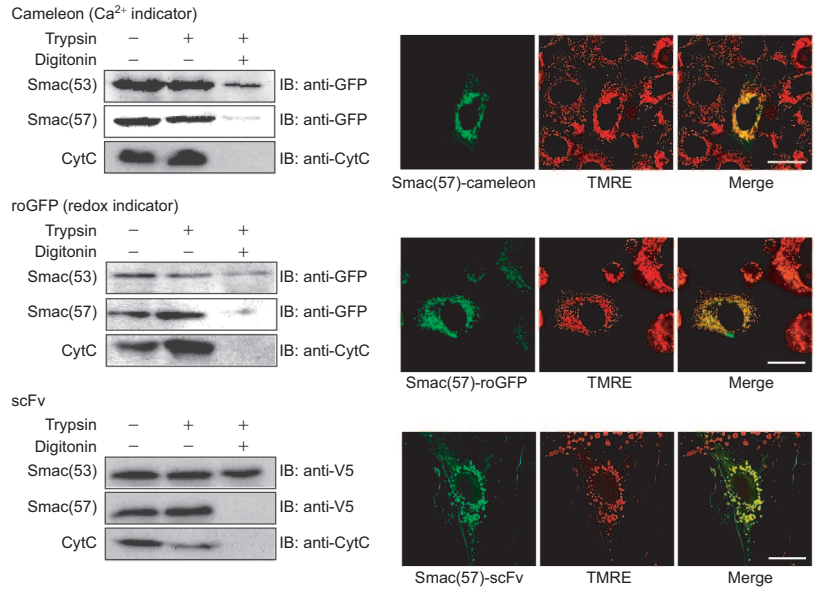

Figure 7. Analysis of exogenous protein localization in submitochondrial compartments. BNL1ME cells transfected with plasmids of the signal-sequence-tagged cameleon, roGFP, and scFv were cultured for 2 d. Mitochondria in the cells were extracted and treated with trypsin and digitonin. The mitochondria were then analyzed by Western blot. Smac(53) and Smac(57) are the proteins connected with the N-terminal 53 and 57 amino acid residues of Smac/DIABLO, respectively. Fluorescence images on the right show the localization of Smac(57)-tagged cameleon, roGFP, and scFv in mitochondria. Bar = 10 μm.

analyzed under otherwise identical conditions. Western blot analysis of the mitochondrial components after subfractionation revealed that cameleon, roGFP, and scFv connected with the IMS-targeting sequence were completely digested in the presence of trypsin and digitonin, whereas those proteins with the matrix-targeting sequence were partially reduced. From these results and the fluorescence images, we conclude that the sequence of the N-terminal 57 amino acids of Smac/DIABLO is generally able to deliver these proteins into the IMS.

Significance of the IMS Targeting Signal and the Identifying Method. Our discovery of the signal sequence will be of great help in resolving the unknown functions of the mitochondrial IMS. We showed that the sequence readily directs any proteins into the IMS without disrupting physiological environments in the IMS. The physiological processes in the IMS are poorly understood, because no method has been known for targeting probes into the IMS. In addition, intracellular expression of engineered antibody fragments, as designed for high-affinity binding reagents, has the potential to inactivate target proteins by modifying or blocking the proteins involved in essential cellular signaling pathways (*18, 19*). Therefore, the signal sequence of the IMS that we identified will become a powerful tool for targeting various probe molecules and intrabodies into the IMS.

It has been reported that the mitochondrial targeting sequence of Smac/DIABLO is similar to that of cytochrome b_2 (Cytb_2) and cytochrome c_1 (Cytc_1) (*22*). The sequences of Smac/DIABLO, Cytb_2, and Cytc_1 consist of bipartite-targeting signal sequences; the mitochondrial-matrix-targeting sequence is followed by the IMS sorting sequence. The matrix-targeting sequence locates a short region of the amino terminus, which forms a basic amphipathic helix. The basic helix is recognized by receptors of the Tom followed by one inner mitochondrial translocase (TIM23 complex). After the helix translocates into the mitochondrial matrix, the IMS sorting sequence is arrested by the TIM23 complex and is then guided into the inner membrane. We have demonstrated that the basic amino acid of Arg10 in Smac/DIABLO is necessary for targeting the mitochondria and that deletion of residues Met1 to Arg10 from the signal sequence causes the protein to lose the ability to target the mitochondria. Four basic amino acids reside in the region from Arg10 to Arg21, so this area is crucial for the formation of the basic amphipathic helix recognized by the Tom and TIM23 complexes. The IMS sorting sequence of Smac/DIABLO is predicted to consist of hydrophobic residues (from 32 to 53), preceded by the three positively charged residues, Lys29-Lys30-Arg31 (*22*). A clear difference exists between the predicted sorting sequence and the results in this paper: while the predicted sorting sequence spans amino acid residues from 32 to 53, the present studies showed that the sequence is insufficient for targeting Smac/DIABLO into the IMS and it functions as a mitochondrial-matrix-targeting sequence. We found that four amino acid residues of Ala-Val-Pro-Ile following the hydrophobic residues are necessary for targeting Smac/DIABLO into the IMS. In addition, we demonstrated that the mutation of either M50K or C53R in all mutants mislocates them to the mitochondrial matrix, possibly because the hydrophobicity of the mutated amino acid residues 32–53 becomes lower than that of the wild-type residues. These results strongly suggest that the hydrophobicity of amino acid residues 32–53 connecting with Ala-Val-Pro-Ile is required to arrest the translocation in the TIM23 complex.

The minimal sequence we found is one of the specific IMS-targeting sequences embedded in the Smac/DIABLO. Most of the region in the sequence was found to be the mitochondrial targeting sequence. For a true minimal sequence of the IMS to be identified, further optimization may be necessary through the elimination of several amino acids in the sequence to shorten the IMS-targeting sequence 10–57 in Smac/DIABLO.

It is well known that a region from Met1 to Cys53 in Smac/DIABLO is processed by the mitochondrial IMP complex (*22*). The signal sequence from Met1 to Ile57 that we identified, therefore, partly overlaps with the N-terminal amino acid sequences of the mature Smac/DIABLO. In contrast, Cytb_2 that has been well identified is separated from the mature IMS proteins by the processing site: mitochondrial-matrix-targeting sequences followed by IMS sorting sequences are completely cleaved. Smac/DIABLO is therefore different from Cytb_2 in that the IMS targeting signal overlaps with the region of the mature protein (*vide supra*).

From a methodological viewpoint, genetic screening from mutation libraries with the present split-EGFP reporter reconstitution should be applicable to any protein of interest as well as Smac/DIABLO as demonstrated in this study. This methodology will

also allow the discovery of specific amino acids and domains that are important for locating an interesting protein in a particular subcellular compartment. We have previously reported that the split-EGFP reporter can be used to identify ER targeting proteins by locating the split half of EGFP in the ER (*39*). The procedure that we have demonstrated will enable the determination of which amino acids of a target protein are essential to target to the ER and to be destined for the Golgi body, lysosome, and extracellular membranes. The split-EGFP reporter is also useful for detecting protein–protein interactions in living cells (*40, 41*). The reporter is readily reconstituted to fluoresce through protein splicing without the need for further transcription, and thus the interactions can be monitored anywhere in the cells. Hence, the reporter for protein–protein interactions in combination with functional screening of mutation libraries will elucidate the critical roles of specific amino acids and domains. Split-EGFP-based functional screening of mutation libraries will therefore provide new insights into defining detailed mechanisms through structure–function analyses.

METHODS

Construction of Plasmids. The cDNAs encoding the fusion proteins of the N-terminal half of EGFP (1–157 amino acids) and the N-terminal DnaE were described previously (*28*). At the C-terminus, the FLAG epitope (DYKDDDDK) was attached when the cDNA was amplified by PCR. The PCR product was subcloned into the pMX vector, which was designated pMX-ED–FLAG. cDNAs of Smac, CaM, and MTS derived from subunit VIII of cytochrome *c* oxidase were subcloned into the pMX-ED–FLAG to produce a fusion gene of pMX-Smac/ED–FLAG, pMX-CaM/ED–FLAG, and pMX-MTS/ED–FLAG, respectively. Each plasmid was transfected into a retrovirus packaging cell line named Platimum-E (PlatE) with Lipofectamine Plus (Invitrogen). After 2 d of culture, high-titer retroviruses were collected and stored at −80 °C before use.

Preparation of BNL1MEims Cells. A cDNA fragment encoding the C-terminus of DnaE and EGFP (amino acids 158–238) was amplified by PCR as a template pMX-MTS/DEc(neo) (*28*). A GN flexible linker $(A(GN)_3GGA(GN)_3GGAG(GN)_3GG)$ was created by PCR. These two PCR products were ligated and subcloned into pBluescript (Stratagene). The fusion gene and a Smac/DIABLO cDNA amplified by PCR were subcloned into the pMX vector. Finally, a neomycin resistance gene connected with an internal ribosome entry site sequence was inserted into the pMX vector. The plasmid thus constructed was transfected into the packaging cell line PlatE. After 2 d of culture, high-titer retroviruses were collected and infected into BNL1ME cells. The cells stably expressing the fusion protein consisting of Smac/DIABLO, DnaEc, and EGFPc were obtained after 14 d of selection in G418 (Invitrogen) containing a growth medium. The cells were subcloned, and a cell line that expressed the fusion protein in mitochondria was obtained.

Fractionation of Mitochondria. Mitochondria were suspended in a sucrose buffer (0.25 M sucrose, 5 mM EDTA, 20 mM Tris/HCl, pH 7.4) in the presence or absence of 0.05% digitonin, or 0.1% Triton X-100 and incubated on ice for 30 min. After the incubation, mitochondria were treated with trypsin (50 $\mu g\ mL^{-1}$) on ice for 10 min and reisolated by centrifugation (10,000 × *g*, 5 min, 4 °C). Mitochondria thus isolated were washed with the sucrose buffer containing 0.2 mM of phenylmethylsulfonyl fluoride. Samples were then lysed in a buffer containing 1% SDS, 10% glycerol, 10% 2-mercaptoethanol, and 50 mM Tris/HCl (pH 6.8) and analyzed by SDS-PAGE.

Western Blot Analysis. Cell lysates or subfractionated mitochondria were electrophoresed with 15% polyacrylamide gels, transferred to nitrocellulose membranes, and blotted with the following antibodies: mouse anti-GFP (Roche Applied Science), goat anti-Tom20 (Santa Cruz Biotechnology), mouse anti-cytochrome *c* (PharMingen), mouse anti-Hsp60 (PharMingen), FLAG (Sigma), and V5 (Invitrogen). The blotted membranes were incubated with alkaline phosphatase-conjugated secondary antibodies and visualized by chemiluminescence (New England Biolabs).

Construction of Mutation Libraries. Random mutation was introduced according to the previously described method (*42*). Briefly, the Smac/DIABLO cDNA was amplified by PCR in the presence of 0.5 mM or 0.2 mM $MnCl_2$. The rate of mutation was determined by the percentage of the number of mutated bases over the total number of the Smac/DIABLO DNA ($n = 10$). The resulting PCR products were trimmed with *Bam*HI and *Not*I and subcloned into pMX-ED–FLAG with those enzyme sites. The libraries were transformed into competent DH10B cells (Invitrogen). The sizes of the libraries were 3.3×10^4 colony forming units (cfu) for Smac(H)/ED–FLAG and 3.7×10^4 cfu for Smac(L)/ED–FLAG.

Sorting and Identifying Smac/DIABLO Mutants. Plasmids encoding the mutant libraries were transfected into the PlatE cells, and retroviruses were collected after 2 d of culture. The retroviral libraries were infected into BNL1MEmito cells with an infection efficiency of 10% as determined by a control experiment using pMX-EGFP. The cells were incubated for 5 d at 37 °C. The cells were stripped off with trypsin–EDTA and resuspended in phosphate-buffered saline (PBS). Fluorescent cells were sorted by FACS and collected on 48-well microplates. To recover Smac/DIABLO cDNAs from the collected cells, we extracted the genome from each BNL1MEmito clone and subjected it to PCR with a pair of PCR primers: 5′-AGGACCTTACACAGTCCTGCTGACC-3′ (forward) and 5′-GCCCTCGCCGGACACGCTGAACTTG-3′ (reverse). The resulting fragments were directly sequenced by an automatic sequencer.

pH Measurements in the IMS. A cDNA of YFP(H148G) connected with the N-terminal 57 residues of Smac/DIABLO was inserted into the pMX vector, and it was transfected into PlatE cells. Retroviruses were collected 2 d after the transfection and infected into NIH3T3 cells with an infection efficiency of 30%. The cells were incubated for 2 d at 37 °C. The cells were stripped off with trypsin–EDTA and resuspended in modified Krebs–Ringer buffer (KRB; 5 mM NaCl, 125 mM KCl, 1 mM Na_3PO_4, 1 mM $MgSO_4$, and 10 mM HEPES) adjusted to the pH values from 7.02 to 7.92. When the pH values were 8.22 and 8.53, Tris was used instead of HEPES. Two ionophores, monensin (5 μM) and nigericin (5 μM), were added to the KRB before the cells were suspended. To generate a standard curve, we used FACS in the differing pH values to analyze the cells infected with the retroviruses and determined mean fluorescence intensities as described (*12*). Independently, the cells infected with the retro-

viruses were stripped off and resuspended in PBS. Fluorescence intensities of the cells were measured by FACS, and the mean fluorescence intensity was estimated.

Digital Imaging of Apoptotic Cells. HeLa cells and MCF7 cells cultured on glass-bottom dishes were transfected with cDNA of YFP(H148G) that was fused with full-length Smac/DIABLO or the N-terminal 53 residues or N-terminal 57 residues of Smac/DIABLO. The cells were incubated for 2 d at 37 °C, and the cells were treated for 6 h with 1 μM STS according to the method previously described (*43*). Images were acquired with a fluorescence microscope IX71 (Olympus) and a 40× 1.30 numerical aperture (NA) oil objective with a 100-W mercury arc lamp for illumination. Digital images were acquired with a cooled electron multiplying CCD camera (iXon, ANDOR Technology) with Meta Morph software (Universal Imaging Corp.).

Identification of YFP(H148G), Cameleon, roGFP, and scFv in Mitochondrial Subcompartments. Each cDNA sequence of amino acid numbers 1–53 and 1–57 in Smac/DIABLO was connected with the cDNAs of YFP(H148G), cameleon, roGFP, and scFv and inserted into the pcDNA3.1 vector (Invitrogen). The vectors were transfected in BNL1ME cells, and the cells were collected 2 d after transfection. Mitochondria were collected according to the methods described above. To blot the YFP(H148G), cameleon, and roGFP, we used anti-GFP antibody, whereas for scFv, we used anti-V5 antibody.

Acknowledgment: This work has been supported by the Japan Society for the Promotion of Science and the Japan Science and Technology Corp. and by grants from the New Energy Industrial Technology Development Organization and the Uehara Memorial Foundation.

Supporting Information Available: This material is free of charge *via* the Internet.

REFERENCES

1. Neupert, W., and Brunner, M. (2002) The protein import motor of mitochondria, *Nat. Rev. Mol. Cell Biol. 3*, 555–565.
2. Rehling, P., Brandner, K., and Pfanner, N. (2004) Mitochondrial import and the twin-pore translocase, *Nat. Rev. Mol. Cell Biol. 5*, 519–530.
3. Truscott, K. N., Brandner, K., and Pfanner, N. (2003) Mechanisms of protein import into mitochondria, *Curr. Biol. 13*, R326–R337.
4. Allen, S., Lu, H., Thornton, D., and Tokatlidis, K. (2003) Juxtaposition of the two distal CX3C motifs *via* intrachain disulfide bonding is essential for the folding of Tim10, *J. Biol. Chem. 278*, 38505–38513.
5. Curran, S. P., Leuenberger, D., Oppliger, W., and Koehler, C. M. (2002) The Tim9p-Tim10p complex binds to the transmembrane domains of the ADP/ATP carrier, *EMBO J. 21*, 942–953.
6. Curran, S. P., Leuenberger, D., Leverich, E. P., Hwang, D. K., Beverly, K. N., and Koehler, C. M. (2004) The role of Hot13p and redox chemistry in the mitochondrial TIM22 import pathway, *J. Biol. Chem. 279*, 43744–43751.
7. Lu, H., Allen, S., Wardleworth, L., Savory, P., and Tokatlidis, K. (2004) Functional TIM10 chaperone assembly is redox-regulated *in vivo*, *J. Biol. Chem. 279*, 18952–18958.
8. Lutz, T., Neupert, W., and Herrmann, J. M. (2003) Import of small Tim proteins into the mitochondrial intermembrane space, *EMBO J. 22*, 4400–4408.
9. Terziyska, N., Lutz, T., Kozany, C., Mokranjac, D., Mesecke, N., Neupert, W., Herrmann, J. M., and Hell, K. (2005) Mia40, a novel factor for protein import into the intermembrane space of mitochondria is able to bind metal ions, *FEBS Lett. 579*, 179–184.
10. Zhang, J., Campbell, R. E., Ting, A. Y., and Tsien, R. Y. (2002) Creating new fluorescent probes for cell biology, *Nat. Rev. Mol. Cell Biol. 3*, 906–918.
11. Abad, M. F., Di Benedetto, G., Magalhaes, P. J., Filippin, L., and Pozzan, T. (2004) Mitochondrial pH monitored by a new engineered green fluorescent protein mutant, *J. Biol. Chem. 279*, 11521–11529.
12. Matsuyama, S., Llopis, J., Deveraux, Q. L., Tsien, R. Y., and Reed, J. C. (2000) Changes in intramitochondrial and cytosolic pH: early events that modulate caspase activation during apoptosis, *Nat. Cell Biol. 2*, 318–325.
13. Llopis, J., McCaffery, J. M., Miyawaki, A., Farquhar, M. G., and Tsien, R. Y. (1998) Measurement of cytosolic, mitochondrial, and Golgi pH in single living cells with green fluorescent proteins, *Proc. Natl. Acad. Sci. U.S.A. 95*, 6803–6808.
14. Filippin, L., Abad, M. C., Gastaldello, S., Magalhaes, P. J., Sandona, D., and Pozzan, T. (2005) Improved strategies for the delivery of GFP-based Ca2+ sensors into the mitochondrial matrix, *Cell Calcium 37*, 129–136.
15. Hanson, G. T., Aggeler, R., Oglesbee, D., Cannon, M., Capaldi, R. A., Tsien, R. Y., and Remington, S. J. (2004) Investigating mitochondrial redox potential with redox-sensitive green fluorescent protein indicators, *J. Biol. Chem. 279*, 13044–13053.
16. Holliger, P., and Hudson, P. J. (2005) Engineered antibody fragments and the rise of single domains, *Nat. Biotechnol. 23*, 1126–1136.
17. Reinman, M., Jantti, J., Alfthan, K., Keranen, S., Soderlund, H., and Takkinen, K. (2003) Functional inactivation of the conserved Sem1p in yeast by intrabodies, *Yeast 20*, 1071–1084.
18. Biocca, S., and Cattaneo, A. (1995) Intracellular immunization: antibody targeting to subcellular compartments, *Trends Cell Biol. 5*, 248–252.
19. Caron de Fromentel, C., Gruel, N., Venot, C., Debussche, L., Conseiller, E., Dureuil, C., Teillaud, J. L., Tocque, B., and Bracco, L. (1999) Restoration of transcriptional activity of p53 mutants in human tumour cells by intracellular expression of anti-p53 single chain Fv fragments, *Oncogene 18*, 551–557.
20. Du, C., Fang, M., Li, Y., Li, L., and Wang, X. (2000) Smac, a mitochondrial protein that promotes cytochrome c-dependent caspase activation by eliminating IAP inhibition, *Cell 102*, 33–42.
21. Verhagen, A. M., Ekert, P. G., Pakusch, M., Silke, J., Connolly, L. M., Reid, G. E., Moritz, R. L., Simpson, R. J., and Vaux, D. L. (2000) Identification of DIABLO, a mammalian protein that promotes apoptosis by binding to and antagonizing IAP proteins, *Cell 102*, 43–53.
22. Burri, L., Strahm, Y., Hawkins, C. J., Gentle, I. E., Puryer, M. A., Verhagen, A., Callus, B., Vaux, D., and Lithgow, T. (2005) Mature DIABLO/Smac is produced by the IMP protease complex on the mitochondrial inner membrane, *Mol. Biol. Cell 16*, 2926–2933.
23. Liu, Z., Sun, C., Olejniczak, E. T., Meadows, R. P., Betz, S. F., Oost, T., Herrmann, J., Wu, J. C., and Fesik, S. W. (2000) Structural basis for binding of Smac/DIABLO to the XIAP BIR3 domain, *Nature 408*, 1004–1008.
24. Chai, J., Du, C., Wu, J. W., Kyin, S., Wang, X., and Shi, Y. (2000) Structural and biochemical basis of apoptotic activation by Smac/DIABLO, *Nature 406*, 855–862.
25. Wu, G., Chai, J., Suber, T. L., Wu, J. W., Du, C., Wang, X., and Shi, Y. (2000) Structural basis of IAP recognition by Smac/DIABLO, *Nature 408*, 1008–1012.
26. Cyr, D. M., Ungermann, C., and Neupert, W. (1995) Analysis of mitochondrial protein import pathway in Saccharomyces cerevisiae with translocation intermediates, *Methods Enzymol. 260*, 241–252.
27. Fuller, K. M., and Arriaga, E. A. (2003) Advances in the analysis of single mitochondria, *Curr. Opin. Biotechnol. 14*, 35–41.
28. Ozawa, T., Sako, Y., Sato, M., Kitamura, T., and Umezawa, Y. (2003) A genetic approach to identifying mitochondrial proteins, *Nat. Biotechnol. 21*, 287–293.
29. Paulus, H. (2000) Protein splicing and related forms of protein autoprocessing, *Annu. Rev. Biochem. 69*, 447–496.

30. Schneider, H., Sollner, T., Dietmeier, K., Eckerskorn, C., Lottspeich, F., Trulzsch, B., Neupert, W., and Pfanner, N. (1991) Targeting of the master receptor MOM19 to mitochondria, *Science 254*, 1659–1662.
31. Stuart, R. A., and Neupert, W. (1990) An exceptional mitochondrial precursor protein using an exceptional import pathway, *Biochimie 72*, 115–121.
32. Cheng, M. Y., Hartl, F. U., Martin, J., Pollock, R. A., Kalousek, F., Neupert, W., Hallberg, E. M., Hallberg, R. L., and Horwich, A. L. (1989) Mitochondrial heat-shock protein hsp60 is essential for assembly of proteins imported into yeast mitochondria, *Nature 337*, 620–625.
33. Stark, G. R., and Gudkov, A. V. (1999) Forward genetics in mammalian cells: functional approaches to gene discovery, *Hum. Mol. Genet. 8*, 1925–1938.
34. Grimm, S. (2004) The art and design of genetic screens: mammalian culture cells, *Nat. Rev. Genet. 5*, 179–189.
35. Neylon, C. (2004) Chemical and biochemical strategies for the randomization of protein encoding DNA sequences: library construction methods for directed evolution, *Nucleic Acids Res. 32*, 1448–1459.
36. Wachter, R. M., Elsliger, M. A., Kallio, K., Hanson, G. T., and Remington, S. J. (1998) Structural basis of spectral shifts in the yellow-emission variants of green fluorescent protein, *Structure 6*, 1267–1277.
37. Cortese, J. D., Voglino, A. L., and Hackenbrock, C. R. (1992) The ionic strength of the intermembrane space of intact mitochondria is not affected by the pH or volume of the intermembrane space, *Biochim. Biophys. Acta 1100*, 189–197.
38. Miyawaki, A., Llopis, J., Heim, R., McCaffery, J. M., Adams, J. A., Ikura, M., and Tsien, R. Y. (1997) Fluorescent indicators for Ca^{2+} based on green fluorescent proteins and calmodulin, *Nature 388*, 882–887.
39. Ozawa, T., Nishitani, K., Sako, Y., and Umezawa, Y. (2005) A high-throughput screening of genes that encode proteins transported into the endoplasmic reticulum in mammalian cells, *Nucleic Acids Res. 33*, e34.
40. Ozawa, T., Nogami, S., Sato, M., Ohya, Y., and Umezawa, Y. (2000) A fluorescent indicator for detecting protein-protein interactions *in vivo* based on protein splicing, *Anal. Chem. 72*, 5151–5157.
41. Ozawa, T., Takeuchi, T. M., Kaihara, A., Sato, M., and Umezawa, Y. (2001) Protein splicing-based reconstitution of split green fluorescent protein for monitoring protein-protein interactions in bacteria: improved sensitivity and reduced screening time, *Anal. Chem. 73*, 5866–5874.
42. Cirino, P. C., Mayer, K. M., and Umeno, D. (2003) Generating mutant libraries using error-prone PCR, *Methods Mol. Biol. 231*, 3–9
43. Rehm, M., Dussmann, H., and Prehn, J. H. (2003) Real-time single cell analysis of Smac/DIABLO release during apoptosis, *J. Cell Biol. 162*, 1031–1043.